J. Fluid Mech. (1965), *vol.* 22, *part* 4, *pp.* 721–735
Printed in Great Britain

Particle motion in laminar vertical tube flow

By R. C. JEFFREY AND J. R. A. PEARSON
Department of Chemical Engineering, Pembroke Street, Cambridge

(Received 15 December 1964)

Some experimental results are presented for the motion of small rigid spherical particles suspended in a Newtonian viscous liquid flowing under steady laminar conditions in a vertical tube of circular cross-section. When the particles were neutrally buoyant, the Segré & Silberberg (1961, 1962) effect was confirmed, the particles moving into a narrow annular zone with a diameter about two-thirds of the tube diameter. When the particles were slightly denser than the fluid, they migrated relatively rapidly to the wall of the tube for downward fluid flow and to the axis of the tube for upward fluid flow. Individual particle trajectories were obtained (necessarily approximately) from photographic records, and statistical techniques used to obtain 'universal' paths for given flow conditions. A complete set of relevant dimensionless parameters is given by the tube flow Reynolds number, the ratio of the tube diameter to the particle diameter, and the ratio of the Stokes free-fall velocity of the particle to the maximum fluid velocity. An attempt has been made to study the dependence of the trajectories on each of these parameters, the ranges being 10–200, 10–20 and 0–0·2 respectively. Detailed results can be found in Jeffrey (1964). Some comments are made on the relevance for this situation of certain theoretical solutions given elsewhere.

1. Introduction

Segré & Silberberg (1961, 1962) have reported, for dilute suspensions of neutrally buoyant rigid spherical particles in a Newtonian liquid moving in Poiseuille flow in tubes, an unexpected effect that had previously been overlooked or wrongly interpreted. By means of a numerous series of experiments, they showed that particles migrate, admittedly slowly, into a thin annular region concentric with the tube axis at a radius about 0·6 of the tube radius. Their method depended essentially on observation of the number of particles passing through fixed cross-sections of the tube, as a function of the radius. Although admirably suited to giving statistical information about large numbers of particles, this technique still left some uncertainty as to the paths traced out by particular particles. The method we have used involved following individual particles by direct photographic means. Because of the very slow migratory movement in neutral density experiments, the errors in our observations have been relatively large; however, by combining the trajectories of several particles under otherwise fixed conditions, we have been able to obtain statistically significant smoothed particle paths.

In attempting to obtain exactly neutrally buoyant conditions for spherical particles, we noticed that slight differences in density between particles and fluid

led to totally different and much more rapid migratory velocities, and we have investigated a few selected cases. For these the errors in observation were relatively less important and so fewer observations at fixed conditions were necessary to establish smooth particle paths. The results we present here are thought to be essentially new, though recent work by Eichhorn & Small (1964) and Repetti & Leonard (1964) overlaps to some extent. The results of Oliver (1962) and Goldsmith & Mason (1962, 1964) are also relevant.

The physical variables defining the flow at any instant of time, t, are:

R the radius of the tube
a the radius of the particle
V_0 the fluid velocity on the tube axis
μ the viscosity of the fluid
ρ_f the density of the fluid
ρ_p the density of the particle
g the acceleration of gravity
(r, θ, z) cylindrical polar co-ordinates relative to an origin on the tube axis
(u_r, u_θ, u_z) the velocity components of the fluid in the (r, θ, z) co-ordinate system
(r_p, θ_p, z_p) the co-ordinates of the centre of a given particle
(V_r, V_θ, V_z) the velocity components of the centre of the particle
$(\omega_r, \omega_\theta, \omega_z)$ the angular velocity components of the particle

Significant variables are shown in figure 1.

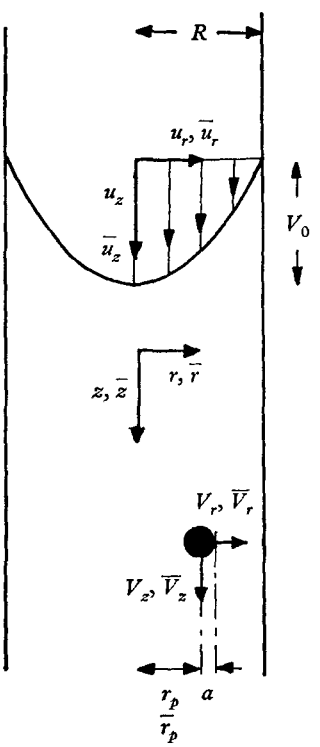

FIGURE 1. Co-ordinate system.

Because of the symmetry of the flow, we shall suppose that

$$u_\theta = V_\theta = \omega_r = \omega_z = 0,$$

and that V_r, V_z and ω_θ are functions of r and z only. These assumptions require only that the flow be laminar, which will be true provided that the tube Reynolds number,

$$Re_T = \rho_f V_0 R/\mu, \tag{1}$$

be smaller than about 2000. If, however, we suppose that the flow is also 'slow' (a term that must be explained later in more detail), then we can assume that inertia forces act as *perturbations* to the flow that would occur according to the Stokes (linearized) equations. For these linearized flow equations, it may be shown (Saffman 1956; Happel & Brenner 1958; Brenner 1962, 1964; Bretherton 1962; Cox 1964) that spheres do not experience transverse forces and so $V_r = 0$ also. This has been verified experimentally by Goldsmith & Mason (1961) for very slow flows. In order to assess the effects of the non-linear terms, we can define three further Reynolds numbers, a particle Reynolds number

$$Re_P = \rho_f V_0 a/\mu = Re_T a/R, \tag{2}$$

a shear Reynolds number, based on the mean shear in the fluid and the particle radius,

$$Re_S = \rho_f V_0 a^2/R\mu = Re_T a^2/R^2, \tag{3}$$

and a free-fall Reynolds number

$$Re_F = \rho_f V_F a/\mu, \tag{4}$$

where

$$V_F = 4a^2(\rho_p - \rho_f)g/18\mu \tag{5}$$

is the Stokes free-fall velocity. If we now define the dimensionless variables

$$\left.\begin{array}{llll} \bar{r} = r/R, & \bar{z} = z/R, & \bar{V}_F = V_F/V_0, & \\ \bar{r}_p = r_p/R, & \bar{z}_p = z_p/R, & \bar{t} = tV_0/R, & \\ \bar{u}_r = u_r/V_0, & \bar{u}_\theta = u_\theta/V_0, & \bar{u}_z = u_z/V_0, & \\ \bar{V}_r = V_r/V_0, & \bar{V}_z = V_z/V_0, & \omega = \omega_\theta R/V_0, & \end{array}\right\} \tag{6}$$

then the relevant equations of motion and boundary conditions can be written in terms of the co-ordinates $(\bar{r}, \theta, \bar{z})$ and $(\bar{r}_p, \theta_p, \bar{z}_p)$, the velocities $(\bar{u}_r, \bar{u}_\theta, \bar{u}_z)$ and $(\bar{V}_r, \bar{V}_z, \omega)$, the time $\bar{t}$ and the three Reynolds numbers Re_T, Re_P and Re_F defined earlier. (The dimensionless ratio $P = a/R = Re_P/Re_T$ can be used as an alternative to Re_P, while $\bar{V}_F$ can take the place of Re_F.)

In the absence of any particles, the tube flow is given by

$$\bar{u}_r = u_\theta = 0, \quad \bar{u}_z = (1-\bar{r}^2); \tag{7}$$

to a first approximation, where all Reynolds numbers and P are small we suppose that the motion of any particle is given by

$$\bar{V}_r = 0, \quad \bar{V}_z = \bar{u}_z(\bar{r}_p) = 1-\bar{r}_p^2, \quad \omega = -r_p; \tag{8}$$

the result for ω follows fairly readily from a solution of Stokes's equations; migratory effects are thought of as being due to small changes in the 'solution' (8), so that

$$\bar{V}_r = \bar{v}_r, \quad \bar{V}_z = 1-\bar{r}_p^2+\bar{v}_z, \quad \omega = -\bar{r}_p+\omega_1, \tag{9}$$

where $\bar{v}_r$, $\bar{v}_z$ and ω_1 are functions of Re_T, Re_P and Re_F and of the various

co-ordinates.† We now further assume that in the second approximation these functions are dependent only on the co-ordinate $\bar{r}_p$ and not on $\bar{z}_p$ or $\bar{t}$ explicitly i.e. that the flow is always quasi-steady or, equivalently, that the terms involving $(\partial/\partial\bar{t})$ in the dimensionless equations of motion are not appreciable compared with the non-linear inertia terms.

We shall not attempt to develop these plausible assumptions theoretically but use them to interpret our observations. Indeed, our experiments were made with the object first of determining whether and when these assumptions held and secondly to obtain what information we could about the dependence of the function $\bar{v}_r$ on $\bar{r}_p$, Re_T, Re_P and Re_F. A brief description of the apparatus and experimental technique is given in § 2, the results are presented in § 3 and the relevance of certain analytic asymptotic solutions is discussed in § 4.

2. Apparatus and experimental technique

A schematic lay-out of the apparatus is shown in figure 2. The tube in which all experiments were performed was a vertical glass tube about 150 cm long and of internal diameter 3·25 cm; the axis of the tube departed from the vertical by less than $\frac{1}{2}$ mm over its entire length and tests showed that the inner surface was of uniform diameter. The test section, 130 cm long, was formed by surrounding the tube by two Perspex boxes, each 60 cm long and 8 cm square, filled with aqueous glycerol solution of refractive index 1·44, the index for the glass tube being 1·475. Since the fluid used for the experiments was also an aqueous glycerol solution of about the same refractive index, this meant that optical distortion in viewing particles through the tube/box arrangement was small ($< 0{\cdot}02$ cm in position for uncorrected photographs). A 16 mm Pathe ciné camera was used to record the passage of particles through the test section.

The particles used were selected from a batch of white polymethyl-methacrylate spheres of a nominal diameter of $\frac{1}{8}$ in. One (hemispherical) half of each particle was very thinly sprayed with black paint. The density of the particles was measured to be 1·193 g/cm^3 in the temperature range 18–23 °C. The particles used were of three sizes: (i) a group with diameter in the range 0·288–0·293 cm chosen directly from the full batch, (ii) a group of diameter $0{\cdot}201 \pm 0{\cdot}002$ cm, and (iii) a group of diameter $0{\cdot}150 \pm 0{\cdot}001$ cm; the latter two groups being obtained by grinding down particles of the largest size. The physical properties of the glycerol/water mixtures used for the suspending fluid were taken from Miner & Dalton (1953), the precise composition being determined by refractometry.

A 'Mono' pump was used to obtain closed-circuit operation, the pump being particularly suited to handling dilute suspensions of spheres in a fluid of the viscosity used (this was in the range 10–50 cP) and of providing a steady pressure gradient. Because the viscosity of the fluid was highly sensitive to temperature changes, as near isothermal conditions as could be achieved were required within the test section; to do this, a heat exchanger was built into the circuit and the

† We shall expect $\bar{v}_r$, v_z and ω_1 to go to zero with P, i.e. with Re_P for $Re_F \boxminus 0$; the Simha (1936) result puts $\bar{v}_z = -\frac{8}{3}P^2$.

system run until steady temperature conditions were achieved. Temperature control proved to be the chief source of experimental difficulty.

Particle injectors were placed above and below the test section and were designed to inject a particle at any required position on a tube diameter at right angles to the plane formed by the tube axis and the camera.

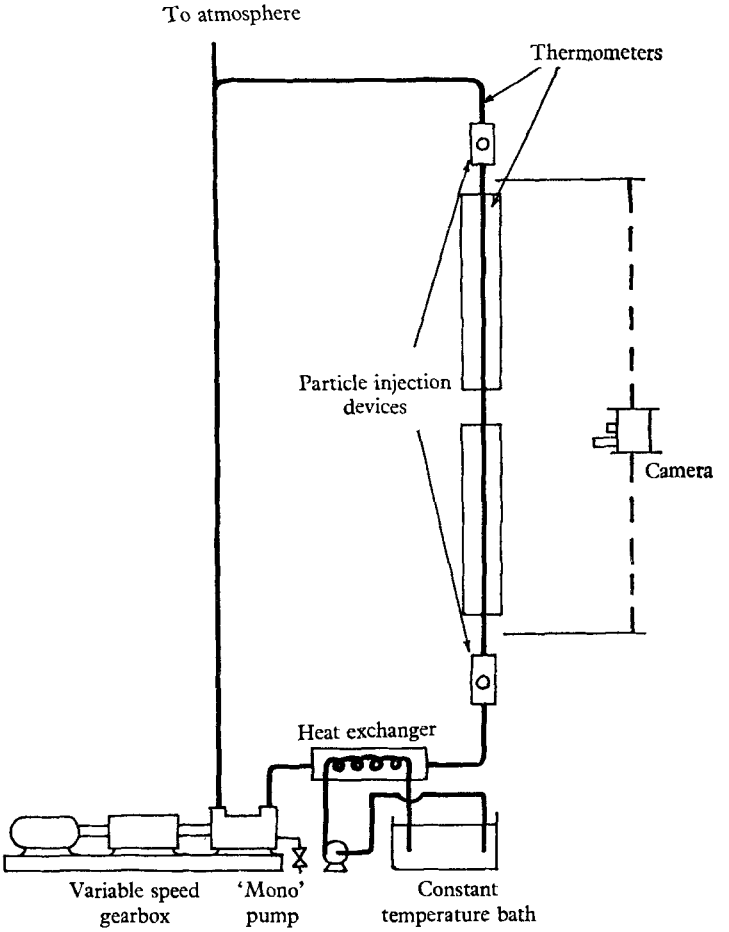

FIGURE 2. Schematic lay-out of apparatus.

Successive frames on ciné film provided the basic information about particle trajectories. By simple measurement on negatives (or projected enlargements thereof), sets of data in the form

$$t_m, z_m, r_m, \phi_m \quad (m = 1, 2, \ldots, n) \tag{10}$$

could be obtained for each particle. Here t_m, z_m and r_m have their obvious significance, while ϕ_m represents the angle of rotation of the spherical particle about its axis of rotation.† Using the notation of § 1,

$$\phi_m - \phi_1 = \int_{t_1}^{t_m} \omega_\theta \, dt. \tag{11}$$

† ϕ_m information was not, and indeed could not be, included for every particle, but only for those for which the black–white interface was suitably oriented initially.

Information about fluid velocity, in particular about V_0, in any set of steady conditions could be obtained by studying the trajectories either of very small air bubbles or of very small particles, other authors (Goldsmith & Mason 1961) having shown that, to the accuracy involved here, these move with the fluid. Values of V_0 were obtained in this way. The data sets (10) were transferred into encoded punched paper tape and were then analysed on the Department's I.B.M. 1620 computer. 'Best fitting' analytic functions, usually polynomial expansions, of the form

$$z = Z(t), \tag{12}$$

$$r = B(t), \tag{13}$$

$$r = C(z), \tag{14}$$

were obtained by standard methods for each particle. By differentiation, we could obtain estimates for the velocity components

$$V_z \simeq dZ/dt, \tag{15}$$

$$V_r \simeq dB/dt; \tag{16}$$

similarly the angular velocity was obtained from

$$\omega_\theta \simeq \delta\phi/\delta t, \tag{17}$$

the δ notation indicating that direct numerical differentiation was employed. A check on (15) and (16) was provided by

$$V_r/V_z \simeq dC/dz. \tag{18}$$

We next *assumed* that, for fixed Re_T, Re_P and Re_F, V_z and V_r were functions of r only, and so by choosing origins for t and z suitably, we could expect to fit *all* data points for *all* particles (using particles of one particular size and under fixed flow conditions) by a 'universal' function. This was done for each group of particles. Standard statistical tests could then be employed to decide whether such universal functions were significantly worse fits to any given particle path than the individual fitted functions. In the case of neutrally buoyant particles, we decided that universal curves were valid and further that observed axial velocity was the best evidence for estimating $\bar{r}_p$.

Finally we attempted, in a purely empirical way, to combine universal curves for various Re_T, Re_P and Re_F by means of dimensionless scaling according to powers of the various Reynolds numbers. However, as these proved to have little evident dynamical validity, they will only be mentioned in passing.

3. Results

3.1. *Rotation of particles*

We compared, for a selection of particles, the angular velocity with which they rotated with the vorticity that the fluid would have had at the position of the centroid in the absence of the particle, i.e. we sought to verify the relation

$$\omega \simeq \tfrac{1}{2}(d\bar{u}_r/d\bar{r})_{\bar{r}=\bar{r}_p} = -\bar{r}_p. \tag{19}$$

Dimensionless plots are shown in figure 3 for various values of Re_T and Re_F with Re_T/Re_P, i.e. P, constant. For the case of neutrally buoyant particles,

figure 3(*c*), some systematic departure was observed, the particles rotating some 7 % more slowly than might be predicted. But for the 'denser' particles, the departures from equation (19) were not significant (in a statistical sense), bearing in mind the inaccuracy of measurement.

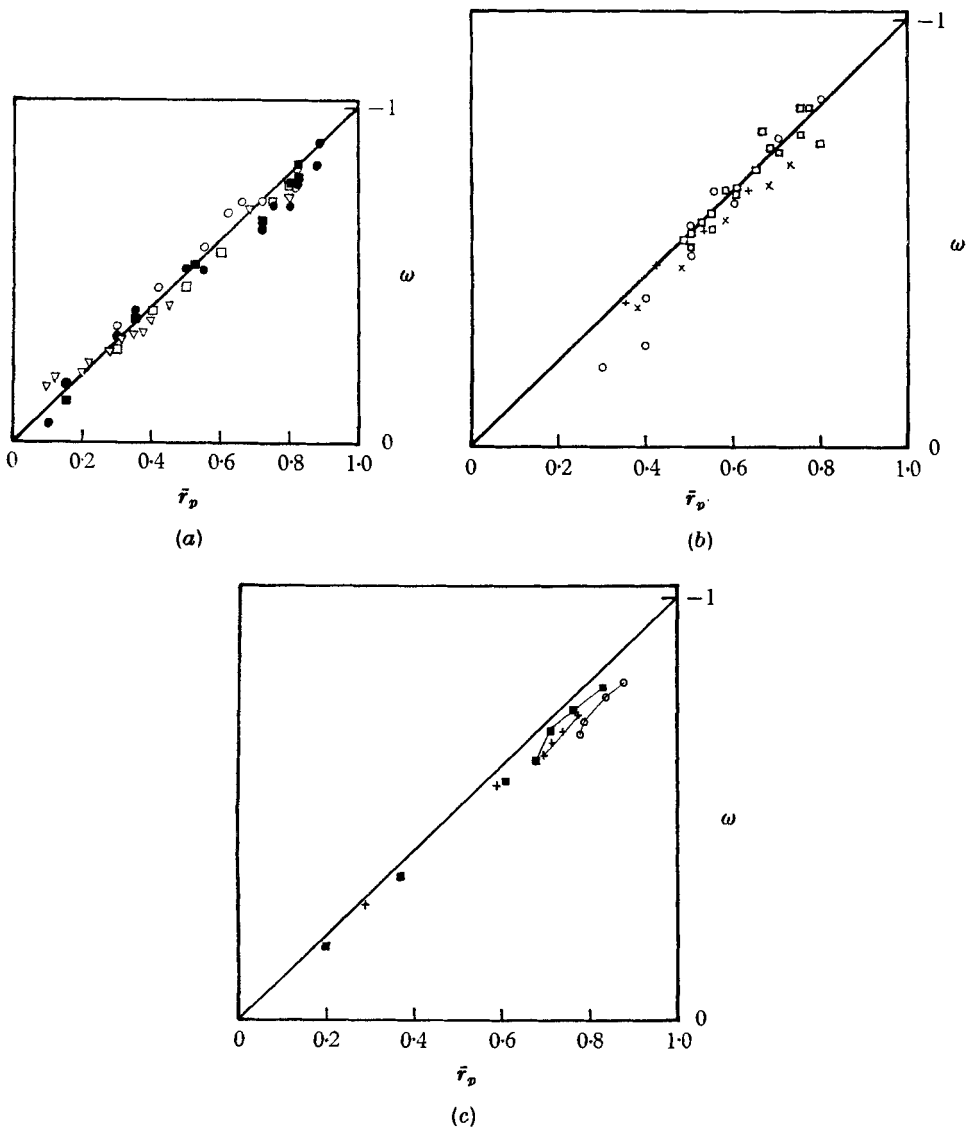

FIGURE 3. Angular velocity ω vs. $\bar{r}_p$. $2a = 0{\cdot}291$ cm; $P = 0{\cdot}09$; —, $\omega = -\bar{r}_p$. (*a*) Dense particles, downward flow: ●, $Re_F = 0{\cdot}545$, $Re_T = 45{\cdot}2$; ■, $Re_F = 0{\cdot}545$, $Re_T = 89{\cdot}8$; ○, $Re_F = 0{\cdot}147$, $Re_T = 22{\cdot}7$; □, $Re_F = 0{\cdot}147$, $Re_T = 59{\cdot}1$; ▽, $Re_F = 0{\cdot}147$, $Re_T = 116$. (*b*) Dense particles, upward flow: ○, $Re_F = 0{\cdot}147$, $Re_T = 22{\cdot}0$; +, $Re_F = 0{\cdot}147$, $Re_T = 49{\cdot}6$; □, $Re_F = 0{\cdot}147$, $Re_T = 113$. (*c*) Neutrally buoyant particles: ○, $Re_T = 11{\cdot}2$; +, $Re_T = 33{\cdot}8$; ■, $Re_T = 72{\cdot}2$.

3.2. *Axial velocity of particles*

Neutrally buoyant particles

Figure 4 shows values of V_z that were calculated according to (15) for various particles. For convenience V_z has been plotted against $(1-\bar{r}^2)$, the straight lines representing the corresponding undisturbed fluid $u_z(\bar{r}_p)$, deduced from observation of small tracer particles. Representative, usually extreme, values of V_z for each particle are shown. The scatter was assumed to be due largely to errors in measuring $\bar{r}_p$, and so it was decided to try using V_z $(=V_0\overline{V}_z)$ as a measure of $\bar{r}_p$ according to $\overline{V}_z = (1-\bar{r}_p^2)$.

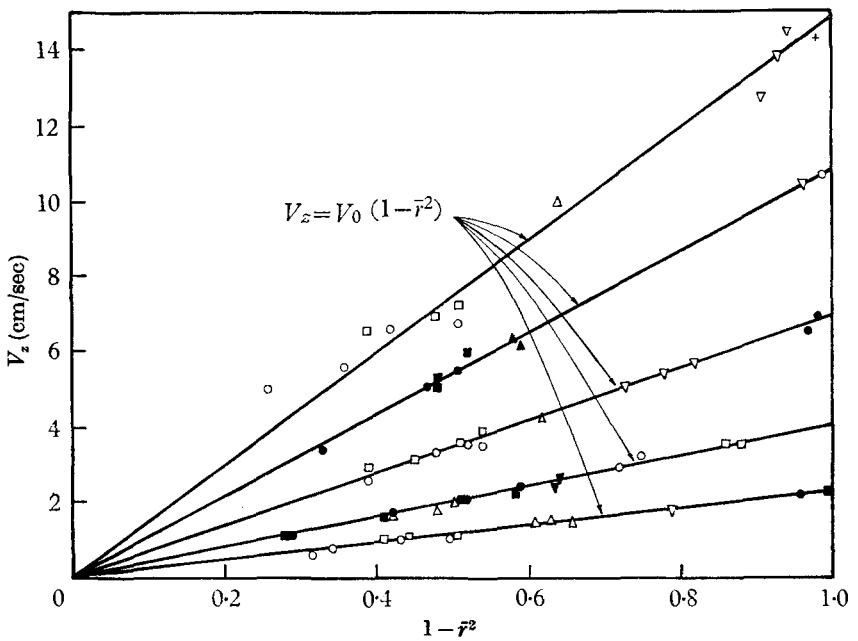

FIGURE 4. Axial velocity V_z vs. $1-\bar{r}_p$ for neutrally buoyant particles. $2a$ = 0·291 cm; P = 00·9. Different symbols close to any line refer to different particles.

Figure 5 shows $(\bar{r}_p)_{\text{obs.}}$ plotted against $(\bar{r}_p)_{\text{calc.}}$ together with expected maximum possible errors. At the same time, we plotted $\overline{V}_z - \overline{u}_z$ against $(\bar{r})_{\text{obs.}}$ (see figure 6) together with expected maximum possible errors. This curve also shows the values of $\overline{V}_z - \overline{u}_z$ that would be expected according to Simha (1936) and more recently to Repetti & Leonard (1964, based on results provided by Goldsmith & Mason). It is seen that all lie within the range of experimental inaccuracy. For convenience, we decided to use $(\bar{r}_p)_{\text{calc.}}$ rather than $(\bar{r}_p)_{\text{obs.}}$ when investigating $\overline{V}_r$ for later experiments—it was an estimate of the latter function that formed the primary object of the investigation.

Dense particles

In this case the value of the function $\overline{V}_z - \bar{v}_z$ was much larger than in the case of the neutrally buoyant particles; indeed it was a primary variable. Figure 7 shows V_z plotted against $1-\bar{r}^2$ for two cases (with various Re_T and Re_F, but with

P fixed): (a) where the net gravitational force on the particle was in the same direction as the mean flow, i.e. downwards, (b) where the mean flow was in the opposite direction, i.e. upwards. In case (a) the particles moved towards the walls

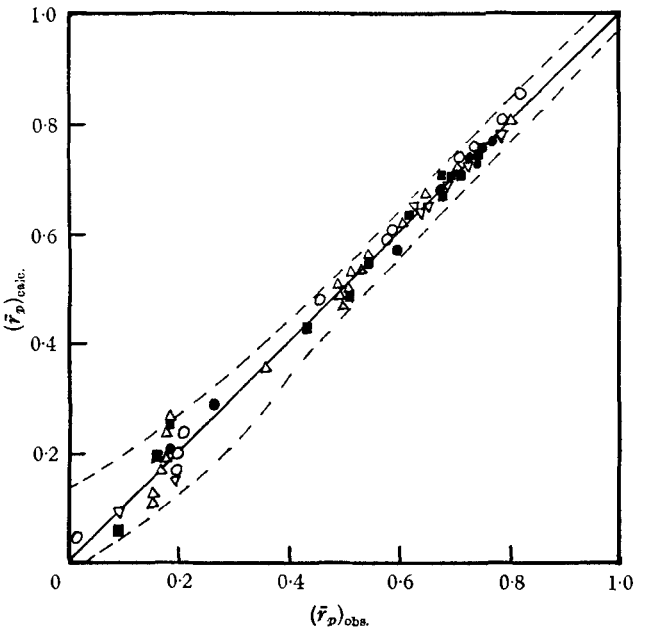

FIGURE 5. Calculated and observed radial positions for neutrally buoyant particles. Different symbols refer to different particles.

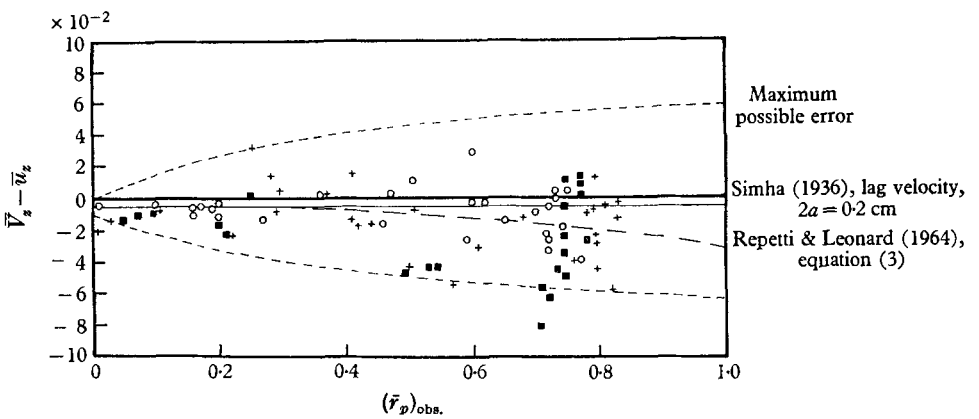

FIGURE 6. Axial velocity lag $\bar{V}_z - \bar{u}_z$ vs. $(\bar{r}_p)_{\text{obs.}}$ for neutrally buoyant particles: ○, $2a = 0{\cdot}291$ cm, $P = 0{\cdot}090$; ■, $2a = 0{\cdot}201$ cm, $P = 0{\cdot}062$; +, $2a = 0{\cdot}150$ cm, $P = 0{\cdot}046$.

of the tube, $1-\bar{r}^2 = 0$, and in case (b) towards the axis, $1-\bar{r}^2 = 1$. Also included are tentative straight lines, which suggest strongly that the particles do not fall through the flowing fluid with the free-fall velocity $\bar{V}_F$ (see equation (6)) but with a relative velocity

$$\bar{V}_R = \bar{V}_F(1-\bar{r}^2). \tag{20}$$

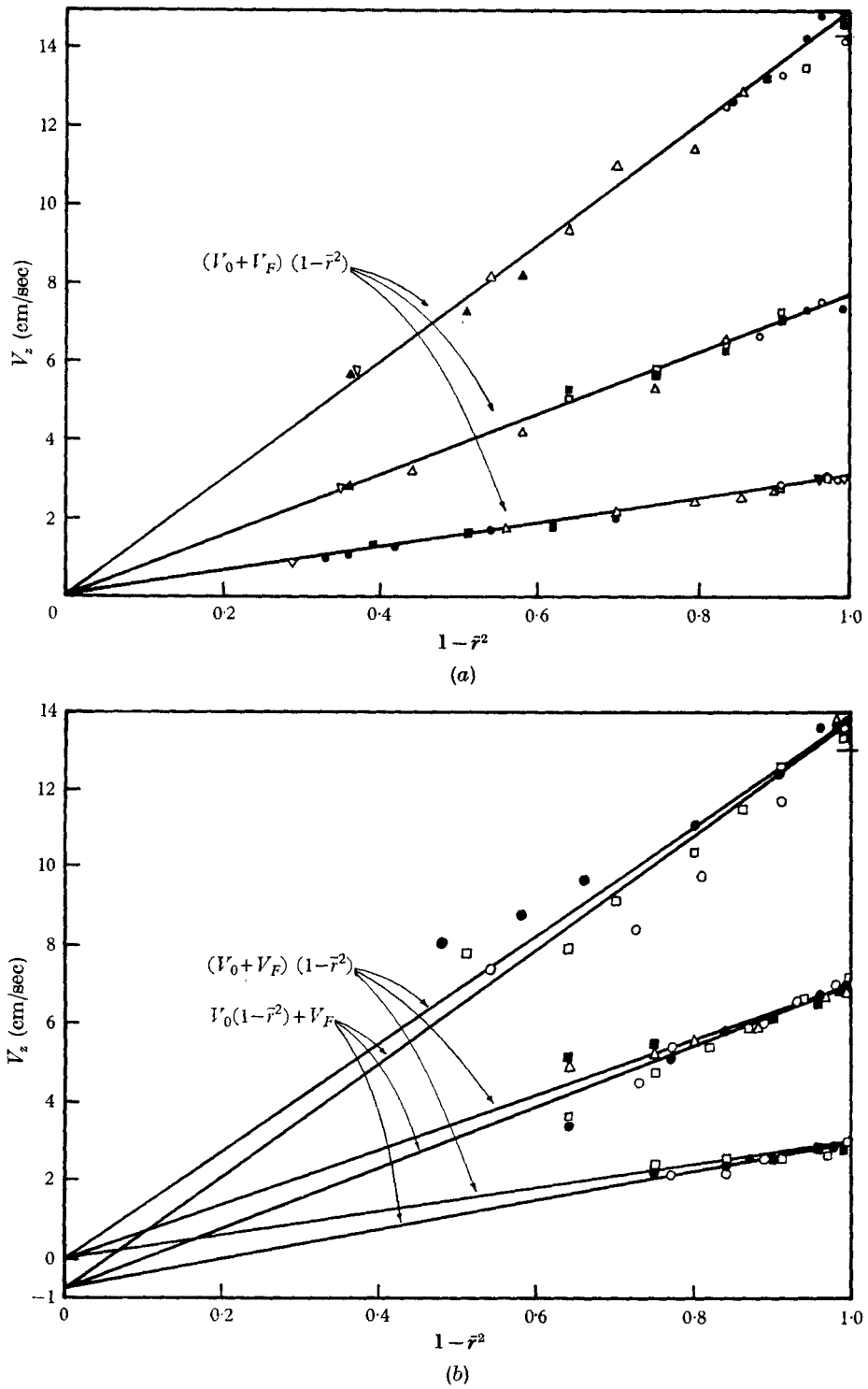

FIGURE 7. Axial velocities (V_z) for dense particles: $2a$ = 0·291 cm; P = 0·09. (*a*) Downward flow, V_F = 0·21 cm/sec, Re_F = 0·147; (*b*) upward flow, V_F = 0·78 cm/sec, Re_F = 0·545.

The scatter of the points in figure 7(*b*) is caused partly by entry (injection) effects—the particles moved so rapidly to the axis that it was difficult to observe many particles with low values of $1-\bar{r}^2$. Nevertheless, it appeared that there may be some systematic difference between cases (*a*) and (*b*). We do not have sufficient information at this stage to say how this behaviour depends upon P, nor can we present any satisfactory explanation for the form of equation (20).

3.3. *Radial velocity of particles*

Neutrally buoyant particles

The velocities in this case were very slow and so any one particle migrated only a short distance during its passage through the observation chamber. As explained above in § 3.2, we decided that axial velocity was as good a measure of radial position as direct observation, and indeed consistent values of $\bar{V}_r$ were

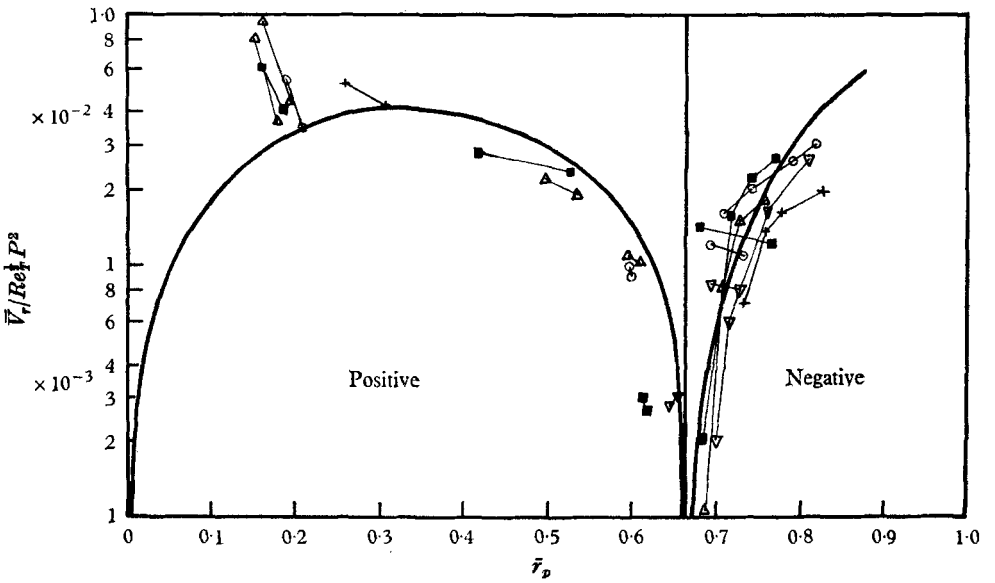

FIGURE 8. Radial velocity plotted as $\bar{V}_r(Re_T)^{-\frac{1}{2}}P^{-2}$ vs. $\bar{r}_p$. Neutrally buoyant particles. $2a = 0{\cdot}291$ cm; $P = 0{\cdot}09$; ○, $Re_T = 11{\cdot}2$; △, $Re_T = 19{\cdot}6$; ■, $Re_T = 33{\cdot}8$; ▽, $Re_T = 52{\cdot}3$; +, $Re_T = 72{\cdot}2$.

obtained on this basis. Figure 8 presents results for P fixed and Re_T varying between 10 and 80. A good empirical correlation was obtained by plotting $\bar{V}_r(Re_T)^{-\frac{1}{2}}P^{-2}$ against $\bar{r}_p$, rather than $\bar{V}_r(Re_T)^{-1}$. Figure 9 presents results for a limited range of $\bar{r}_p$ for three values of P; correlation has been obtained by plotting $\bar{V}_r(Re_T)^{-\frac{1}{2}}P^{-2}$ against $\bar{r}_p$. A recent paper by Saffman (1965), which came to the authors' notice *after* the empirical correlation had been noted, suggests that this non-integral dependence on Re_T may be genuine. Although Segré & Silberberg suggest that better correlation is obtained using $\bar{V}_r(Re_T)^{-1}P^{-3}$ than by using $\bar{V}_r(Re_T)^{-\frac{1}{2}}P^{-2}$ their experimental evidence barely distinguishes between the two possibilities; this is explained and demonstrated in detail in Jeffrey (1964). A further suggestion (Saffman 1965) that results should be

correlated according to $\overline{V}_r(Re_T)^{-\frac{2}{3}}P^{-3}$ leads to yet another grouping of points that is neither clearly better nor worse than others. It is worth pointing out that the values of Re_T involved are larger here than for Segré & Silberberg's work or for Goldsmith & Mason's. It can therefore be argued that the observations made here are of a situation where terms of higher order than the second (see equation (9)) are dominant.

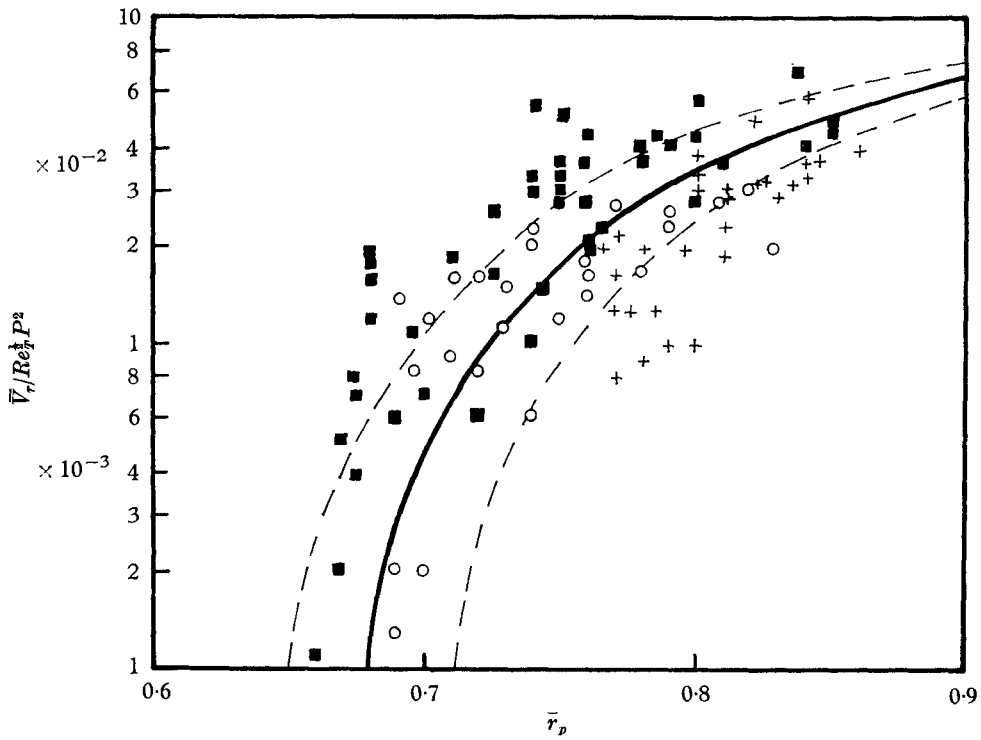

FIGURE 9. Radial velocity plotted as $\overline{V}_r(Re_T)^{-\frac{1}{2}}P^{-2}$ vs. $\bar{r}_p$. Neutrally buoyant particles. ○, $P = 0{\cdot}09$; ■, $P = 0{\cdot}062$; +, $P = 0{\cdot}046$.

Dense particles

The radial velocities were larger in this case and directly calculable from photographs using (16), though smoothed curves from figure 7 were also used to derive $\bar{r}_p$ from V_z data. Figure 10 shows results for case (*a*), downward fluid flow; results are plotted in the form $\overline{V}_r/Re_F P$ against $\bar{r}_p$, this choice of dimensionless scaling having been adopted to correspond with some theoretical predictions of Rubinow & Keller (1961), discussed later.† From a purely empirical point of view, it was found that better correlation was obtained by considering $\overline{V}_r(Re_F)^{-\frac{1}{2}}$. Figure 11 shows corresponding results for case (*b*), upward fluid flow. Although the general pattern in cases (*a*) and (*b*) appeared to be similar, systematic differences could be detected; i.e. for fixed Re_T, Re_F and P, reversing the sign of V_0 seemed to change the magnitude of $\overline{V}_r$ as well as its sign.

† This choice should *not* be thought as implying that the Rubinow & Keller result is to be preferred on theoretical grounds.

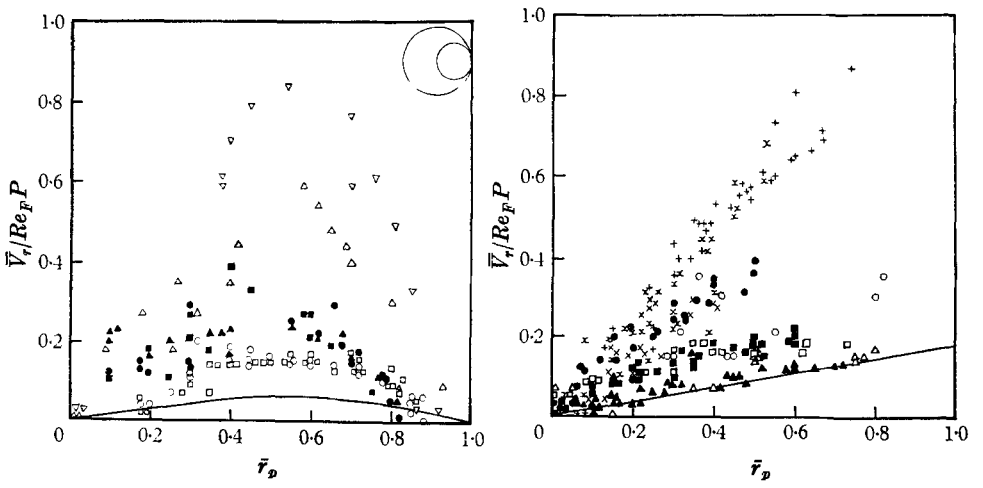

FIGURE 10. Radial velocity, comparison with Rubinow & Keller (1961): $\bar{V}_r/Re_F P$ vs. $\bar{r}_p$. Dense particles.

(*a*) Downward flow: —, $\frac{1}{6}\bar{r}_p(1-\bar{r}_p^2)$.

	P	Re_P	Re_T
○	0·09	0·545	45·2
□	0·09	0·545	89·8
●	0·09	0·147	22·7
■	0·09	0·147	59·1
▲	0·09	0·147	116
△	0·046	0·083	45·3
▽	0·046	0·083	89·0

(*b*) Upward flow: —, $\frac{1}{6}\bar{r}_p$.

	P	Re_P	Re_T
●	0·09	0·545	46·1
■	0·09	0·545	61·3
▲	0·09	0·545	115
○	0·09	0·147	22·0
□	0·09	0·147	49·6
△	0·09	0·147	113
+	0·046	0·083	21·2
x	0·046	0·083	23·9
×	0·046	0·083	52·4

4. Discussion

First, let it be emphasized that the results reported here are not exhaustive, and cannot be more than indicative of the quantitative nature of general particle migration in Poiseuille flow. The qualitative picture is however quite clear. Dense particles falling slowly through an upward moving fluid migrate to the tube axis; buoyant particles in the same flow migrate to the tube wall (though quantitative results for this case have not been given here, the effect has been confirmed). Conversely, dense particles falling through a downward moving fluid migrate to the tube walls and buoyant particles to the tube axis.

The orders of magnitude of the various forces acting must be dependent on the values of the three Reynolds numbers, Re_T, Re_P and Re_F, defined by equations (1), (2) and (4), but it is not at all clear which combinations are relevant for those forces causing migration. All that we can say is that these forces are non-linear (it having been noted in § 1 that linearized equations do not lead to migration), and that if all the Reynolds numbers are sufficiently small, then the observed radial migration will be, to first order, the result of a balance between

these non-linear 'lift' forces and the linear 'Stokes' drag of a particle moving relative to the fluid, i.e.

$$\mu V_0 a[fn(Re_T, Re_P, Re_F, \bar{r}_p)] = \mu V_0 a[6\pi \overline{V}_z]. \tag{21}$$

Thus if we measure the radial velocity $V_0 \overline{V}_z$, use of (21) gives us the lift force. By taking a sufficient number of observations in $(Re_T, Re_P, Re_F, \bar{r}_p)$-space, it might be possible to determine the functional dependence observationally, but this is unlikely to be very rewarding because of the difficulty of getting accurate measurements over a sufficient range of each of the variables. It is likely to prove more profitable in the long run to compare a limited range of observations with a theoretical prediction for lift force, based on asymptotic expansions using solutions of the linearized equations of motion as the first terms of the expansions. Unfortunately no complete expansion procedure including simultaneously the effect of sheared fluid flow, presence of tube walls and gravity forces has yet been attempted; a semi-empirical comparison with the Rubinow & Keller (1961) result for a particle rotating and translating in an otherwise-stationary fluid is one that has been persistently suggested. In this we neglect (!) the parabolic velocity profile of the moving fluid, and use the actual angular velocity ω (see equation (19)) of the particle, and its relative axial velocity $\overline{V}_z - \overline{u}_z$ to evaluate the lift force F_1 according to the relation

$$F_1 = \mu V_0 a[\pi Re_S \omega (\overline{V}_z - \overline{u}_z)]. \tag{22}$$

The 'predictions' for $\overline{V}_r$, using (21) and the observed values for ω and $(\overline{V}_z - \overline{u}_z)$, are shown as full lines in figures 10 (*a*) and (*b*). Although the comparison is hardly convincing, the correspondence between the r-dependence of observed and calculated curves is surprisingly good. Saffman (1965) has shown theoretically that a migratory velocity of the form $\overline{V}_r / Re_F P \doteq 80 \bar{r}_p^{\frac{1}{2}} (Re_T)^{-\frac{1}{2}}$ should in any case dominate the Rubinow & Keller velocity if circumstances were such that either should strictly apply. This value proves to be far too large numerically by comparison with observed results (by a factor of the order of 5 on the ordinate scale of figure 10 (*a*) for $\bar{r}_p = 0{\cdot}5$), but has an acceptable dependence on $\bar{r}_p$ away from the tube walls.

Returning to the question of what constitutes a slow flow, we see that, in all the cases we have reported, the radial migratory velocities lead to very small ($\ll 1$) Reynolds numbers, $\overline{V}_r a \rho_f / \mu$, the free-fall Reynolds numbers Re_F are small (< 1), the particle shear Reynolds numbers Re_S are small (< 1), though the particle Reynolds numbers Re_P are of the order of 1–10. Since it is usually assumed that asymptotic expansions are only likely to lead to useful approximations when the expanding parameter is of order unity or less, it is clearly important to decide what the relevant expansion parameters are, before we can decide whether we are observing a 'slow' flow. The neutrally buoyant results, where $Re_F \equiv 0$, suggest that Re_S or even PRe_S is the relevant quantity for that special situation. By writing $(\overline{V}_z - \overline{u}_z) = O(PRe_F / Re_T)$ relations (22) and (21) suggest that $P^3 Re_F$ is then also relevant for the case of dense particles. The important point seems to be that Re_T can be large, and that Re_P as such may not

have to be small. The effect of Re_T is likely to be a subtle one, in that it may determine which of several essentially separate perturbation effects, each a slow flow in the true sense, is dominant.

REFERENCES

BRENNER, H. 1962 *J. Fluid Mech.* **12**, 35.

BRENNER, H. 1964 *J. Fluid Mech.* **18**, 144.

BRETHERTON, F. P. 1962 *J. Fluid Mech.* **14**, 284.

COX, R. G. 1964 Ph.D. Thesis, University of Cambridge.

EICHHORN, R. & SMALL, S. 1964 *J. Fluid Mech.* **20**, 513.

GOLDSMITH, H. L. & MASON, S. G. 1961 *Nature, Lond.*, **190**, 1095.

GOLDSMITH, H. L. & MASON, S. G. 1962 *J. Coll. Sci.* **17**, 448.

GOLDSMITH, H. L. & MASON, S. G. 1964 *2nd Europ. Conf. Microcirculation, Bibl. Anat.*, **4**, 462.

HAPPEL, J. & BRENNER, H. 1958 *J. Fluid Mech.* **4**, 195.

JEFFREY, R. C. 1964 Ph.D. Dissertation, University of Cambridge.

MINER, C. S. & DALTON, N. M. 1953 *Glycerol.* London: Chapman and Hall.

OLIVER, D. R. 1962 *Nature, Lond.*, **194**, 1269.

REPETTI, R. V. & LEONARD, E. F. 1964 *Nature, Lond.*, **203**, 1346.

RUBINOW, S. I. & KELLER, J. B. 1961 *J. Fluid Mech.* **11**, 447.

SAFFMAN, P. G. 1956 *J. Fluid Mech.* **1**, 540.

SAFFMAN, P. G. 1965 *J. Fluid Mech.* **22**, 385.

SEGRÉ, G. & SILBERBERG, A. 1961 *Nature, Lond.*, **189**, 209.

SEGRÉ, G. & SILBERBERG, A. 1962 *J. Fluid Mech.* **14**, 115, 136.

SIMHA, R. 1936 *Koll. Z.* **76**, 16